Research Square

Preprints are preliminary reports that have not undergone peer review.
They should not be considered conclusive, used to inform clinical practice,
or referenced by the media as validated information.

Evaluating cell free DNA quantification and integrity in breast cancer using fluorometric, electrophoretic and PCR based platforms

Gisha Rose Antony
St. John's Research Institute
Vidya P Nimbalkar
St. John's Research Institute
Sowmya Nagaraj
St. John's Research Institute
S Mahalakshmi
St. John's Research Institute
Anupama C. E
St. John's Research Institute
Ganapathi Bantwal
St.John's Medical College Hospital
Belinda George
St.John's Medical College Hospital
Akshay Ajoy
St. John's Medical College
Nihal M Ahmed
St. John's Medical College
Rakesh S. Ramesh
St.John's Medical College Hospital
Jyothi D. N
St.John's Medical College Hospital
Jayakumari S
St.John's Medical College Hospital
Jyothi S Prabhu
jyothi@sjri.res.in

St. John's Research Institute

Research Article

Keywords: Breast cancer, Cell-free DNA, cfDNA integrity, Liquid biopsy

Posted Date: February 25th, 2026

DOI: https://doi.org/10.21203/rs.3.rs-8794932/v1

License: This work is licensed under a Creative Commons Attribution 4.0 International License.
Read Full License

Additional Declarations: No competing interests reported.

Abstract

Background

Cell-free DNA (cfDNA) has emerged as a promising biomarker for cancer detection and monitoring. However, different quantification and integrity assessment methods may yield variable results. This study aimed to compare cfDNA concentration and integrity between breast cancer (BC) patients and healthy controls using three complementary analytical techniques and to evaluate the concordance between these approaches.

Methods

Plasma cfDNA from BC patients and healthy controls was quantified using Qubit fluorometry, electrophoretic profiling by TapeStation (TS), and ALU-based quantitative PCR (qPCR) assays. cfDNA integrity was assessed using two indices: TS-derived DNA Integrity Index (DII) and ALU-qPCR–derived DII (ALU 247/115 ratio). Spearman correlation analyses were performed to compare results across methods.

Results

cfDNA concentration was significantly elevated in BC patients compared with controls across all three platforms, even after genomic DNA (gDNA) correction. Qubit, TS, and gDNA-corrected cfDNA concentrations showed strong correlations in both groups, indicating robust cross-method agreement. In contrast, cfDNA integrity showed method-dependent differences: ALU-qPCR–derived DII was significantly higher in tumor samples, whereas TS-derived DII did not differ between groups. Moreover, TS DII and ALU-qPCR DII were not correlated, suggesting that the two methods capture distinct aspects of cfDNA fragmentation.

Conclusions

cfDNA quantification is consistent across fluorometric, electrophoretic, and qPCR-based methods. However, cfDNA integrity assessments vary substantially by technique. ALU-qPCR appears more sensitive in distinguishing BC- associated fragmentation patterns. Combining cfDNA quantification with ALU-qPCR-based integrity analysis may enhance the diagnostic utility of cfDNA in BC.

Background

Cell-free DNA (cfDNA) refers to short DNA fragments released into the bloodstream through apoptosis, necrosis, or active cellular secretion. In patients with malignancy, a fraction of this circulating DNA originates from tumor cells (circulating tumor DNA, ctDNA), reflecting tumor dynamics, burden, and

genomic alterations[1–3]. ctDNA is identified within cfDNA by tumor-specific mutations, copy-number variations, gene rearrangements, and methylation signatures[4]. Its ability to detect cfDNA through a simple blood draw has made it a central analyte in liquid biopsy based cancer diagnostics[5]. In breast cancer (BC), elevated cfDNA levels and altered fragmentation profiles have been associated with advanced stage, poor prognosis, and minimal residual disease[6–8], highlighting cfDNA as a potential non-invasive biomarker both for early detection and disease monitoring.

Both the quantitative and qualitative characteristics of cfDNA are informative. The total cfDNA concentration reflects global DNA release and tumor cell turnover[9,10], whereas the cfDNA integrity index (DII), defined as the ratio of long to short DNA fragments, captures the underlying mode of cell death[6,7]. High DII values are often linked to necrosis-driven DNA release from malignant cells, while low DII values are characteristic of the apoptotic fragmentation seen in healthy individuals[7,11,12]. Reliable measurement of cfDNA concentration and integrity is therefore essential for distinguishing tumor-derived cfDNA from background DNA of hematopoietic origin.

However, cfDNA analysis is complicated by methodological diversity. Fluorometric assays such as Qubit quantify total double-stranded DNA rapidly but cannot discriminate cfDNA from contaminating gDNA. Electrophoretic instruments like the Agilent TS visualize cfDNA fragment size distribution, identifying mono- and di/tri-nucleosomal fragments, yet they may fail to detect highly degraded cfDNA[13,14]. In contrast, qPCR assays targeting repetitive elements such as ALU sequences enable sequence-specific quantification and DII calculation (e.g., ALU 247/ ALU 115), offering higher analytical sensitivity[15]. Reported discrepancies among these approaches raise concerns about assay comparability and interpretation of cfDNA-based biomarkers.

Only a limited number of studies have directly compared cfDNA quantification and integrity across multiple analytical platforms, and virtually none have done so in a large, treatment-naïve Indian BC cohort. To address this gap, we performed a systematic comparison of cfDNA concentration and integrity in plasma from BC patients and healthy controls using three complementary techniques, Qubit fluorometry, TS electrophoretic profiling, and ALU-based qPCR. We further incorporated gDNA-correction of fluorometric data and assessed inter-method concordance. This work aims to identify the most reliable and sensitive approach for cfDNA assessment and to provide practical guidance for assay standardization in BC liquid-biopsy research.

Materials and Methods

Patients and Control Samples

Peripheral blood samples were obtained from primary BC patients (n = 100) recruited prior to initiation of any treatment after voluntary consent from participants. Age- and gender-matched healthy individuals (n = 70) were included as normal controls. Study was approved by institutional ethics board. Peripheral

blood samples were collected in EDTA tubes and processed within 2 hours of collection. Plasma was separated by centrifugation at 1300 × g for 10 min at 4°C and carefully aliquoted to avoid cellular contamination. Plasma aliquots were stored at − 80°C in the institute biorepository for prolonged periods until cfDNA extraction. Repeated freeze-thaw cycles were strictly avoided, as they are known to reduce cfDNA yield and promote fragmentation and degradation, as reported in previous studies. No consistent variation in cfDNA concentration attributable to storage duration was observed across samples. The study was conducted between February 2024 and November 2025.

cfDNA Extraction

cfDNA from BC patients and control samples was extracted from 500 µL of plasma using the BioChain Cfpure Cell Free DNA Extraction Kit (# K5011610) according to the manufacturer's instructions. The extracted cfDNA was quantified using the Qubit High Sensitivity (HS) DNA Assay Kit (# Q32851) and stored at − 20°C.

cfDNA Fragmentation Profiling and DII Calculation

The fragmentation profile of cfDNA was analyzed using the TS4150 system (Agilent Technologies, Santa Clara, CA, USA). For each run, 2 µL of extracted cfDNA was mixed with 2 µL of HS D1000 sample buffer (# 5067–5603) in an 8-tube strip. Additionally, 2 µL of the HS D1000 ladder (# 5067–5587) prepared with the sample buffer was loaded into well A1 of the tube strip holder.

Data were processed and analyzed using the TS Analysis Software version 5.1 (Agilent Technologies, Santa Clara, CA, USA). Mononucleosomal fragments (short fragments) were defined as cfDNA fragments ranging from 100 to 300 bp, while di- and tri-nucleosomal cfDNA fragments (long fragments) were defined as fragments between 301 and 1000 bp.

The cfDNA Integrity Index (DII) was calculated using the following formula:

DII=Area under the curve (AUC) of long fragments (301–1000 bp)/AUC of short fragments (100–300 bp)

gDNA correction of the cfDNA total concentration

To obtain a more accurate estimate of cfDNA levels, we corrected the Qubit derived total cfDNA concentration for gDNA contamination. Since the TS electrophoresis profiles provide fragment-size information, we used TS data to estimate the proportion of gDNA contamination in each sample. In the TS electropherogram, the gDNA contribution was quantified as the percentage area corresponding to high-molecular-weight fragments (> 1 Kb), which represents cellular gDNA. This gDNA percentage was then used to adjust the total cfDNA concentration measured by Qubit [16] using the formula:

Corrected cfDNA concentration = Qubit total DNA × (1 – gDNA%)

This correction allowed us to account for variability introduced by sample handling, leukocyte lysis, and differential gDNA release across samples. The corrected cfDNA values are likely to reflect cfDNA population more accurately, ensuring comparability between tumor and control samples.

Estimation of ctDNA concentration and DII by qPCR

The fraction of ctDNA within the total cfDNA was analyzed using ALU-based qPCR assays according to previous method[15]. Briefly, Two ALU repetitive elements, ALU115 (115 bp amplicon) and ALU247 (247 bp amplicon), were quantified using following primer sequences. ALU115 amplified both short and long DNA fragments and measured the total cfDNA content in plasma, whereas ALU247 targeted longer DNA fragments, predominantly released through necrotic processes, and was considered indicative of ctDNA. The primer pair used is as below:

ALU 115 Forward: 5’-CCTGAGGTCAGGAGTTCGAG-3’

Reverse: 5’-CCCGAGTAGCTGGGATTACA-3’

ALU 247 Forward: 5’-GTGGCTCACGCCTGTAATC-3’

Reverse: 5’-CAGGCTGGAGTGCAGTGG-3’

For amplification, 1 µL of template DNA was added to a 10 µL reaction volume containing 3 pM primers. Quantification was performed using SYBR Green master mix (Takara) on the LightCycler 480 II platform (Roche Diagnostics) using the conditions standardized previously[15].

The DNA copy number and the DII, measured by the ratio of ALU247 to ALU115 (ALU247/ALU115), were calculated as described previously[15].

Statistical Analysis

Statistical analyses were performed using R (version 4.5.1) software. Differences in cfDNA concentration and DII between control and tumor groups were assessed using the Mann-Whitney U test. Correlations of cfDNA concentration across different quantification methods, and the correlation of DII obtained by ALU-based qPCR and TS, were evaluated using Spearman’s rank correlation test. p value < 0.05 was considered statistically significant.

Results

cfDNA concentration is elevated in BC patients compared to normal controls

The total cfDNA concentration was estimated using three complementary approaches: Qubit fluorometry, TS electrophoretic profiling, and ALU-based qPCR assays. cfDNA concentrations measured by both Qubit (mean concentration: 0.459 ng/μL in patients and 0.252 ng/μL in controls) and TS (mean concentration: 0.156 ng/μL in patients and 0.090 ng/μL in controls) showed a significant increase in BC patients compared with healthy individuals ($p < 0.0001$ and $p = 0.0048$, respectively; Fig. 1a–b, Supplementary Table 2).

We further evaluated cfDNA concentrations across clinically relevant subgroups, including patients aged > 50 years versus ≤ 50 years, early-stage versus late-stage disease, and molecular subtypes (detailed patient data and clinical characteristics are provided in Supplementary Table 1). Among molecular subtypes, cfDNA yield was highest in HER2-positive tumors (mean concentration: 0.516 ng/μL), followed by hormone receptor–positive tumors (HR+) (0.480 ng/μL) and triple-negative breast cancer (TNBC) (0.298 ng/μL) (Supplementary Fig. 1a). A trend toward higher cfDNA levels was observed in patients aged > 50 years ($p = 0.059$; Supplementary Fig. 1b). Late-stage disease also showed a trend toward higher cfDNA levels compared with early-stage disease ($p = 0.093$; Supplementary Fig. 1c).

The fraction of ctDNA within the total cfDNA was further evaluated using ALU-based qPCR. The DII assessed using the ALU247/115 ratio, was significantly higher in patients relative to controls ($p = 0.0002$; Fig. 1c). A higher DII, along with elevated cfDNA concentrations measured by Qubit and TS, is indicative of an increased ctDNA burden in BC patients.

Together, these findings highlight the utility of multi-platform cfDNA assessment in distinguishing tumor-derived cfDNA signatures from those of healthy controls.

TS profiles showed visible gDNA contamination in both groups

We next evaluated cfDNA fragment distributions in the BC and control groups using TS electrophoretic profiling. The fragment analysis revealed detectable gDNA contamination in both tumor and control samples (Fig. 2a-f). To assess the extent to which gDNA contamination contributed to the measured cfDNA concentrations and the DII values derived from ALU qPCR, we performed gDNA correction on the Qubit-estimated concentrations. After subtracting the gDNA fraction determined from the TS profiles, the corrected cfDNA concentrations remained significantly higher in patients (mean concentration: 0.219 ng/μL in patients and 0.153 ng/μL in controls, $p < 0.0001$, Fig. 2g), indicating that the elevated cfDNA levels in patients were not attributable to gDNA contamination. We further examined the concordance between the different cfDNA quantification approaches. Pairwise correlation analysis demonstrated a strong positive association between cfDNA concentrations measured by Qubit and TS, even after gDNA correction, in both patients and controls (Table 1), indicating robust inter-method concordance in cfDNA quantification across independent analytical platforms. These findings validate the reliability of both fluorometric and electrophoretic quantification for assessing cfDNA burden in plasma samples.

Table 1
Correlation between cfDNA estimation methods in BC patients and control groups by different platforms

Comparison	Spearman's r_s (Tumor)	p-value	Spearman's r_s (Control)	p-value
Qubit vs TS	0.609	**< 0.0001**	0.323	**0.007**
Qubit vs gDNA-corrected cfDNA	0.682	**< 0.0001**	0.834	**< 0.0001**
TS vs gDNA-corrected cfDNA	0.534	**< 0.0001**	0.549	**< 0.0001**

Measurement of cfDNA integrity is method dependent

The fraction of ctDNA within the total cfDNA was evaluated by ALU-based RT-PCR (Fig. 1c) and by TS fragmentation profile. ALU115 captured the total pool of circulating DNA by amplifying both short and long fragments, whereas ALU247 predominantly detected long DNA fragments, which are generally associated with necrosis and enriched in ctDNA. ALU247 levels were significantly higher in BC patients compared to control samples, as shown in Fig. 3a ($p < 0.0001$). In contrast, cfDNA fragmentation profiles derived from TS electropherograms calculated as the ratio of di- and tri-nucleosomal (larger fragments) to mono-nucleosomal DNA (smaller fragment) (DII by L/S), did not differ significantly between tumor and control samples (Fig. 3b, $p = 0.180$). Similarly, concentrations of mono- and di/tri-nucleosomal cfDNA were comparable between groups (Table 2), indicating that both approaches capture distinct biological and technical aspects of cfDNA. TS-based integrity indices are derived from electrophoretic size distribution and primarily reflect nucleosomal fragmentation patterns, which may be less sensitive to minor tumor-specific shifts, especially when tumor burden is low or masked by hematopoietic cfDNA. Correlation analysis between ALU-based DII and TS-derived DII further revealed no significant association (Fig. 3c, $r_s = -0.075$, $p = 0.540$ for controls; $r_s = -0.170$, $p = 0.091$ for tumor samples). ALU247 amplifies sequence-specific fragments that may span sizes overlapping with TS-defined short fragments, whereas TS-based DII is derived purely from electrophoretic size distribution. Hence the correlation reflects fundamental methodological and biological differences, rather than a contradiction between the two approaches emphasizing that PCR-based DII is more sensitive and accurate for detecting subtle changes in cfDNA fragment composition and ctDNA enrichment.

Table 2
Comparison of nucleosomal cfDNA features between patients and controls measured by tapestation (TS).

Parameter	Tumor (mean)	Control (mean)	p-value
Mono-nucleosomal concentration (ng/µl)	0.125 ± 0.168	0.093 ± 0.045	0.212
Di-/tri-nucleosomal concentration (ng/µl)	0.048 ± 0.092	0.034 ± 0.026	0.067
Mono-nucleosomal fragment size (bp)	195.160	202.580	–
Di-/tri-nucleosomal fragment size (bp)	562.820	545.565	–

Discussion

In this study, we systematically compared cfDNA quantification and integrity in BC patients and healthy controls using three complementary approaches: Qubit fluorometry, TS electrophoretic profiling, and ALU-based-qPCR. The total cfDNA concentration was consistently higher in BC patients compared to healthy controls by all three methods, remained significant even after correcting for gDNA contamination. This observation is consistent with previous reports linking elevated cfDNA levels to increased tumor cell turnover, apoptosis, and necrosis in cancer patients[11,17–19]. The pair-wise correlation analysis revealed that the cfDNA concentration measured by three quantification methods were strongly correlated, highlighting the robustness of concentration measurements across analytical platforms. However, when assessing DII, we observed a clear divergence between methods. The DII derived from ALU-based-qPCR was significantly higher in BC patients compared to controls, whereas TS-derived integrity indices did not differ between groups. Moreover, ALU-based DII and TS-DII did not correlate, highlighting the differences in capturing distinct biological and technical features of cfDNA by these two methods. ALU-based-qPCR relies on amplification of repetitive elements of different lengths, with the short fragment (ALU115) reflecting apoptotic cfDNA and the long fragment (ALU247) capturing necrosis-related or gDNA-derived fragments[7,20–22]. Thus, an increased ALU247/115 ratio in tumor patients likely reflects the contribution of necrotic tumor cell death, a hallmark of advanced tumor stage. TS integrity indices are derived from electrophoretic size distribution of cfDNA, focusing primarily on the relative abundance of mono- and di-nucleosomal fragments. This method may be less sensitive to subtle differences in cfDNA fragment origin, particularly if the tumor burden is modest or if the background of hematopoietic cfDNA masks tumor-specific alterations[23,24]. ALU-based-qPCR is a highly sensitive, sequence-specific method capable of detecting small shifts in cfDNA fragment composition. TS, while powerful for visualization and quantification of fragment profiles, may lack the resolution to detect these biological differences. Additionally, pre-analytical variables such as plasma processing, storage, and cfDNA extraction efficiency may disproportionately impact fragment size distributions measured by TS, but not qPCR amplification ratios[25,26]. Our results therefore highlight a critical methodological point: while cfDNA concentration measurements are reproducible across platforms, DII is method-dependent and requires cautious interpretation. The lack of agreement between ALU-based-qPCR and TS does not represent a contradiction but rather reflects their measurement of different biological aspects of cfDNA;

apoptotic/necrotic origin versus physical fragment size distribution. In practical terms, our findings suggest that ALU-based-qPCR may be better suited for distinguishing ctDNA from background cfDNA in the circulation, whereas TS is more useful for assessing overall fragment profiles and detecting large-scale contamination with gDNA. Therefore, we emphasize the need to standardize cfDNA integrity assays before clinical implementation, as relying on a single platform could lead to conflicting conclusions. We further suggest that combining complementary methods, such as total cfDNA concentration with ALU-based-qPCR, may provide a more comprehensive understanding of cfDNA biology and enhance its utility as a biomarker in cancer research. Our data also underscore the importance of correcting for gDNA contamination, which significantly influences fluorometric quantification and may confound downstream analyses.

Conclusion

Taken together, our study demonstrates that cfDNA concentration is a robust marker of tumor presence, but cfDNA integrity requires careful methodological consideration. Future work with additional orthogonal assays, including gDNA correction using single-copy gene[26,27] and next-generation sequencing (NGS) of cfDNA fragmentation patterns, may help to reconcile these discrepancies and establish reliable cfDNA integrity metrics for clinical use.

Abbreviations

cfDNA	Cell-free DNA
ctDNA	Circulating Tumor DNA
DII	DNA Integrity Index
gDNA	Genomic DNA
HER2	Human Epidermal Growth Factor Receptor 2
HR+	Hormone Receptor-Positive
NGS	Next-Generation Sequencing
TS	TapeStation
TNBC	Triple-Negative Breast Cancer

Declarations

Ethics approval and consent to participate

Ethical approval for this study was obtained from the Institutional Ethics Committee (IEC), St. John's Medical College & Hospital, Bengaluru (IEC Study Ref. No.: 252/2023). Informed consent was obtained from all subjects involved in the study.

Consent for publication

Not applicable

Competing interests

The authors declare that they have no competing interests.

Funding

This work was supported by the Indian Council of Medical Research (ICMR) through the grant awarded to Jyothi S Prabhu (ICMR Project ID: IIRP-2023-1560).

Author Contribution

All authors contributed to the study conception and design. Experimental design, execution of experiments, data analysis was performed by G.R.A, V. P. N, S.N and J.S.P. Plasma processing, sample storage, and computational data entry were handled by M.S and A.C.E. G.B, B.G, A.A, N.M.A, J.D.N, and J assisted with recruitment of control participants and manuscript review. R.S.R provided clinical breast cancer samples. The first draft of the manuscript was prepared by G.R.A and J.S.P, and all authors contributed to revising the manuscript. All authors read and approved the final version of the manuscript. J.S.P acquired funding. J, G.B, B.G, and J.S.P supervised the study. All authors approved the final version of the manuscript.

Acknowledgement

The authors are grateful to Nadathur Estates and the Bagaria Education Trust for their support of all the breast cancer research activities at SJRI since 2008.

Data Availability

The data supporting the findings of this study are available with the corresponding author and will be shared upon reasonable request.

References

1. Qin Z, Ljubimov VA, Zhou C, Tong Y, Liang J. Cell-free circulating tumor DNA in cancer. Chin J Cancer. 2016;35(1):36.
2. Tsui WA, Jiang P, Lo YD. Cell-free DNA fragmentomics in cancer. Cancer Cell. 2025.
3. Landon BV, Annapragada AV, Niknafs N, Velculescu VE, Anagnostou V. Liquid biopsies across the cancer care continuum. Nat Med. 2025:1–16.
4. Sobhani N, Generali D, Zanconati F, Bortul M, Scaggiante B. Cell-free DNA integrity for the monitoring of breast cancer: future perspectives? World J Clin Oncol. 2018;9(2):26.
5. Cohen JD, Li L, Wang Y, Thoburn C, Afsari B, Danilova L, et al. Detection and localization of surgically resectable cancers with a multi-analyte blood test. Science. 2018;359(6378):926–30.
6. Madhavan D, Wallwiener M, Bents K, Zucknick M, Nees J, Schott S, et al. Plasma DNA integrity as a biomarker for primary and metastatic breast cancer and potential marker for early diagnosis. Breast Cancer Res Treat. 2014;146(1):163–74.
7. Umetani N, Giuliano AE, Hiramatsu SH, Amersi F, Nakagawa T, Martino S, et al. Prediction of breast tumor progression by integrity of free circulating DNA in serum. J Clin Oncol. 2006;24(26):4270–6.
8. Parsons HA, Rhoades J, Reed SC, Gydush G, Ram P, Exman P, et al. Sensitive detection of minimal residual disease in patients treated for early-stage breast cancer. Clin Cancer Res. 2020;26(11):2556–64.
9. Zhu G, Guo YA, Ho D, Poon P, Poh ZW, Wong PM, et al. Tissue-specific cell-free DNA degradation quantifies circulating tumor DNA burden. Nat Commun. 2021;12(1):2229.
10. Abdelhalim MS, Ahmed MS, Eldabah NA, Khedr G, Elsaid AA. Impact of early changes in circulating cell-free DNA load on outcome in metastatic luminal breast cancer patients. Senses Sci. 2025;12(1):1–13.
11. Lamminaho M, Kujala J, Peltonen H, Tengström M, Kosma VM, Mannermaa A. High cell-free DNA integrity is associated with poor breast cancer survival. Cancers (Basel). 2021;13(18):4679.
12. Iwai T, Yamada T, Uehara K, Shinji S, Matsuda A, Yokoyama Y, et al. Evaluating cell-free DNA integrity index as a non-invasive biomarker for neoadjuvant chemotherapy in colorectal cancer patients. BMC Cancer. 2025;25(1):1153.
13. Jeon K, Lee J, Lee JS, Kim M, Kim HS, Kang HJ, et al. Quantification of cell-free DNA: a comparative study of three different methods. J Lab Med Qual Assur. 2019;41(4):214–9.
14. Sinha SK, Brown H, Knopf K, Hall P, Shannon WD, Haack W. A novel cell-free DNA fragmentomic assay and its application for monitoring disease progression in real time for stage IV cancer patients. Cancers (Basel). 2025;17(21):3583.
15. Nair MG, Ramesh RS, Naidu CM, Mavatkar AD, VP S, Ramamurthy V, et al. Estimation of ALU repetitive elements in plasma as a cost-effective liquid biopsy tool for disease prognosis in breast cancer. Cancers (Basel). 2023;15(4):1054.
16. Alcaide M, Cheung M, Hillman J, Rassekh SR, Deyell RJ, Batist G, et al. Evaluating the quantity, quality and size distribution of cell-free DNA by multiplex droplet digital PCR. Sci Rep.

2020;10(1):12564.
17. Khurram I, Khan MU, Ibrahim S, Saleem A, Khan Z, Mubeen M, et al. Efficacy of cell-free DNA as a diagnostic biomarker in breast cancer patients. Sci Rep. 2023;13(1):15347.
18. Spindler KLG, Pallisgaard N, Andersen RF, Brandslund I, Jakobsen A. Circulating free DNA as biomarker and source for mutation detection in metastatic colorectal cancer. PLoS ONE. 2015;10(4):e0108247.
19. Valpione S, Gremel G, Mundra P, Middlehurst P, Galvani E, Girotti MR, et al. Plasma total cell-free DNA is a surrogate biomarker for tumour burden and a prognostic biomarker for survival in metastatic melanoma patients. Eur J Cancer. 2018;88:1–9.
20. Hussein NA, Mohamed SN, Ahmed MA. Plasma ALU-247, ALU-115, and cfDNA integrity as diagnostic and prognostic biomarkers for breast cancer. Appl Biochem Biotechnol. 2019;187(3):1028–45.
21. Fawzy A, Sweify KM, El-Fayoumy HM, Nofal N. Quantitative analysis of plasma cell-free DNA and its DNA integrity in patients with metastatic prostate cancer using ALU sequence. J Egypt Natl Canc Inst. 2016;28(4):235–42.
22. Park MK, Lee JC, Lee JW, Hwang SJ. Alu cell-free DNA concentration, Alu index, and LINE-1 hypomethylation as a cancer predictor. Clin Biochem. 2021;94:67–73.
23. Saelee SL, Lovejoy AF, Hinzmann B, Mayol K, Huynh S, Harrell A, et al. Quantitative PCR-based method to assess cell-free DNA quality, adjust input mass, and improve next-generation sequencing assay performance. J Mol Diagn. 2022;24(6):566–75.
24. Sathyanarayana SH, Spracklin SB, Deharvengt SJ, Green DC, Instasi MD, Gallagher TL, et al. Standardized workflow and analytical validation of cell-free DNA extraction for liquid biopsy using a magnetic bead-based cartridge system. Cells. 2025;14(14):1062.
25. Krasic J, Abramovic I, Vrtaric A, Nikolac Gabaj N, Kralik-Oguic S, Katusic Bojanac A, et al. Impact of preanalytical and analytical methods on cell-free DNA diagnostics. Front Cell Dev Biol. 2021;9:686149.
26. Nikolaev S, Lemmens L, Koessler T, Blouin JL, Nouspikel T. Circulating tumoral DNA: preanalytical validation and quality control in a diagnostic laboratory. Anal Biochem. 2018;542:34–9.
27. Koessler T, Paradiso V, Piscuoglio S, Nienhold R, Ho L, Christinat Y, et al. Reliability of liquid biopsy analysis: an inter-laboratory comparison of circulating tumor DNA extraction and sequencing with different platforms. Lab Invest. 2020;100(11):1475–84.

Figures

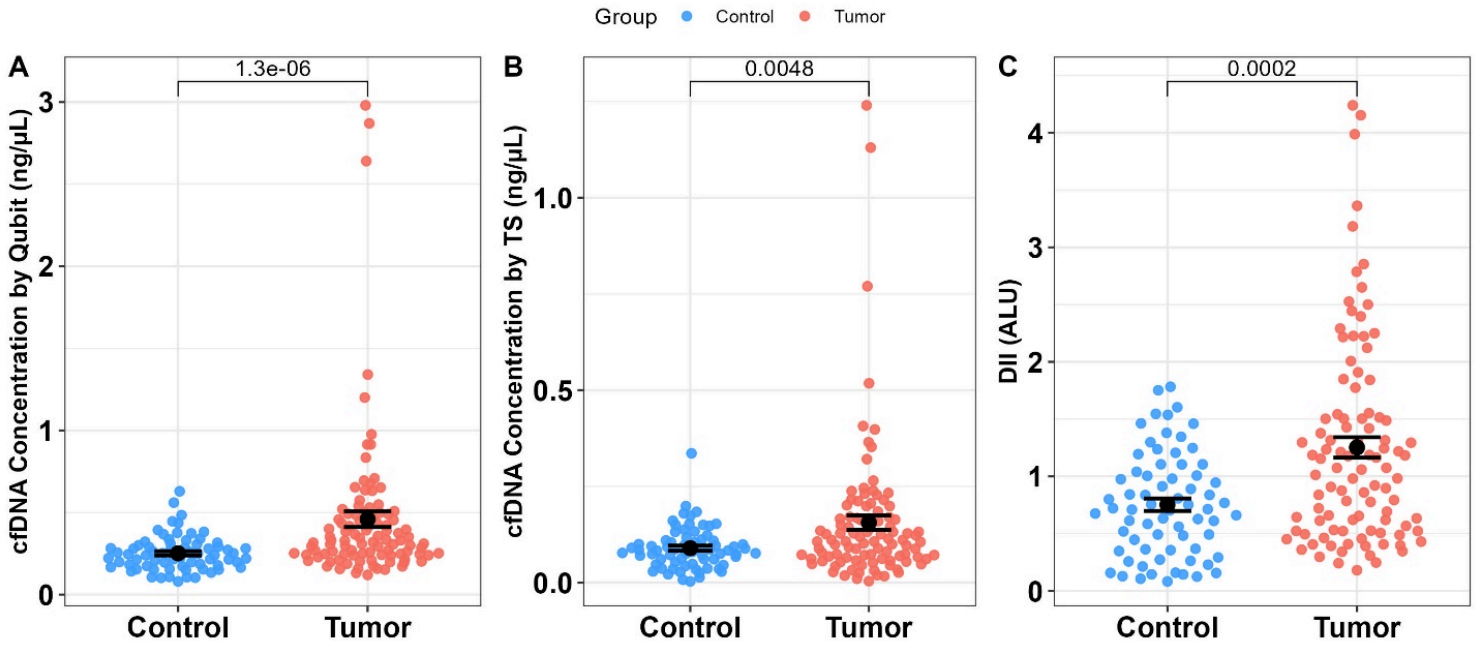


Figure 1

Comparison of cfDNA levels and DII between BC patients and healthy controls.

(a) Total cfDNA concentration measured by Qubit fluorometry shows a significant increase in tumor samples compared to controls ($p<0.0001$). (b) cfDNA concentration estimated by TS electrophoretic profiling also demonstrates higher levels in tumor samples ($p=0.0048$). (c) DII calculated using ALU-based qPCR, is significantly increased in tumor samples, reflecting a higher proportion of longer DNA fragments ($p=0.0002$). Horizontal lines represent mean values; p-values from Mann-Whitney U test are shown.

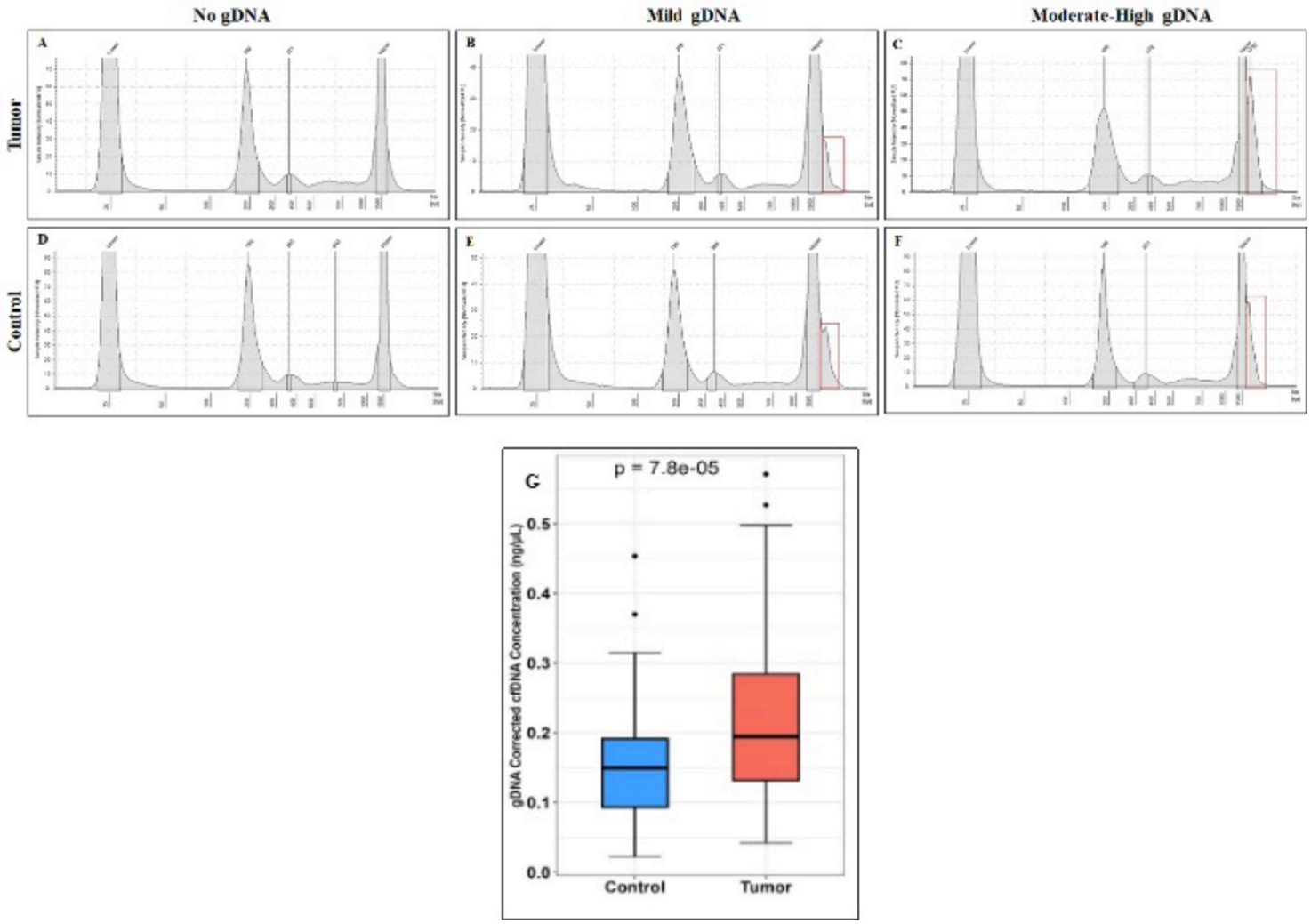


Figure 2

TS fragment profiles and gDNA-corrected cfDNA concentration.

(a-c) Representative TS electropherograms from tumor samples showing cfDNA fragment distributions with prominent mono- and di-nucleosomal peaks and varying degrees of gDNA contamination: no detectable gDNA (a), mild gDNA contamination (b), and moderate-to-high gDNA contamination (c). (d-f) Corresponding electropherograms from control samples showing no detectable gDNA (d), mild gDNA contamination (e), and moderate-to-high gDNA contamination (f). High-molecular-weight gDNA fragments are highlighted by red boxes. (g) gDNA-corrected cfDNA concentrations are significantly higher in tumor samples compared to controls (Mann-Whitney U test; $p < 0.0001$).

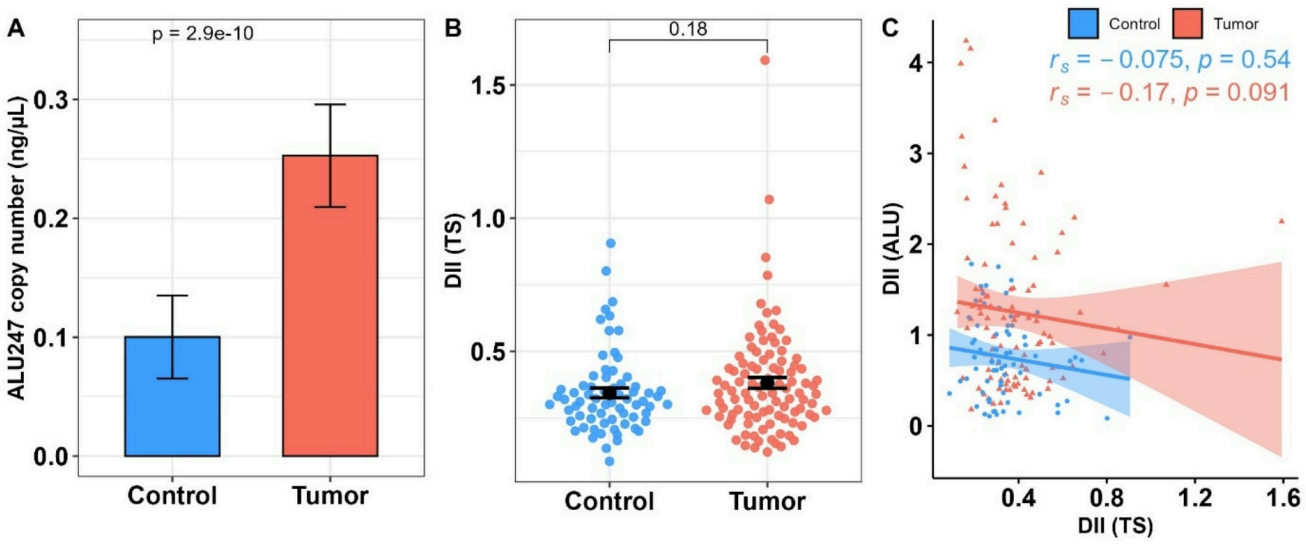


Figure 3

Comparison of qPCR- and TS-derived cfDNA integrity measurements.

(a) Long-fragment cfDNA quantified by ALU247-qPCR is significantly elevated in tumor samples compared to controls ($p < 0.0001$). (b) TS-derived DII (ratio of large to small cfDNA fragments) shows no significant difference between groups (Mann-Whitney U test; $p=0.18$). (c) Correlation analysis demonstrates no association between ALU-based DII and TS-derived DII, indicating method dependency ($r_s = -0.075$, $p = 0.54$ for controls; $r_s = -0.170$, $p = 0.091$for tumor samples).

Supplementary Files

This is a list of supplementary files associated with this preprint. Click to download.

- SupplimentaryFile.pdf